Conference on Modelling Fluid Flow (CMFF'22)
The 18th International Conference on Fluid Flow Technologies
Budapest, Hungary, August 30-September 2, 2022

PERSPECTIVES ON OPENFOAM NUMERICAL SIMULATIONS OF SLOPE WINDS ON MARS

Jose I. ROJAS[1], Santiago ARIAS[1], Adeline MONTLAUR[1]

[1] Dept. of Physics - Division of Aerospace Eng., Universitat Politècnica de Catalunya, c/ Esteve Terradas 7, 08860 Castelldefels, Spain. Tel.: +34 93 413 4130. Fax: +34 93 413 7007. E-mails: santiago.arias@upc.edu, adeline.de.montlaur@upc.edu
[2] Corresponding author. E-mail: josep.ignasi.rojas@upc.edu

ABSTRACT

Planetary boundary layer phenomena, such as slope winds and nocturnal low-level jets, are frequent on Mars, *e.g.*, whenever diurnal surface temperature variations are significant, and large-scale winds are weak. In particular, thermally-driven winds are very common over sloping regions; they can reach significantly high speeds for steep slopes, and govern near-surface winds in many sites. Simulations of this type of flows on Earth have usually been conducted using commercial computational fluid dynamics software (CFD). In this work, a set-up is described for numerically simulating slope flows on Mars within the framework of the open-source code OpenFOAM CFD. For this purpose, thermally-driven winds are analysed in an idealised 2D Martian mountain-valley system with realistic values of parameters such as the slope angle, temperature difference between the atmosphere and slope, etc. The fluid domain dimensions, and the temperature and pressure initial and boundary conditions used in this work were tested and proven suitable in previous similar investigations for Earth applications. Large-eddy simulations (LES) turbulent model is used here. The results obtained for velocity and temperature profiles are shown both for anabatic (up-slope) and katabatic (down-slope) winds. This study shows the potential of the proposed methodology and the performance of OpenFOAM. Future work aims at facilitating the screening of large numbers of candidate landing sites for future Mars missions, and at estimating the thermally-driven wind speeds for wind resource assessment.

Keywords: computational fluid dynamics (CFD), Mars, OpenFOAM, slope winds, thermally-driven winds

NOMENCLATURE

M	[kg/mol]	Molar mass of Martian air
Pr	[−]	Prandtl number
Pr_t	[−]	turbulent Prandtl number
R'	[J/(kg K)]	specific gas ct.
T	[K]	temperature
T_M	[s]	Martian sol period
c_p	[J/(kg K)]	specific heat at ct. pressure
p	[Pa]	static pressure
t	[s]	time
z_0	[m]	roughness length scale
U	[m/s]	flow velocity
u	[m/s]	along-slope velocity
g	[m/s^2]	gravity acceleration
α	[deg]	slope angle
β	[K^{-1}]	volume expansion coef.
μ	[kg/(m s)]	dynamic viscosity
ν	[m^2/s]	molecular kinematic viscosity

Subscripts and Superscripts

x, z	along-slope, slope-normal coordinates
max	maximum
t	turbulent
X, Y, Z	width, depth, and height coordinates

1. INTRODUCTION

Planetary boundary layer (PBL) phenomena such as slope winds and nocturnal low-level jets (LLJ) are frequent on Mars, *e.g.*, whenever diurnal surface temperature variations are significant and large-scale winds are weak [1]. Particularly, thermally-driven winds are very common over sloping regions, may reach high speeds for steep slopes, and govern near-surface winds in many sites. Most of the Earth's PBL modeling approaches are being applied as well to the Martian PBL, including very high-resolution large-eddy simulations (LES) [2], the same way LES have been used on Earth [3, 4]. In particular, numerical simulations of this type of flows on Earth, framed in the atmospheric boundary layer (ABL), have usually been conducted using commercial computational fluid dynamics (CFD) software. Here, the potential of OpenFOAM for simulating

slope flows on Mars is explored, following previous investigations on OpenFOAM turbulence models and temperature and pressure boundary conditions (BC) and initial conditions (IC) for simulating such flows on Earth [5, 6].

This work aims to facilitate, in the future, the screening of large numbers of candidate landing sites for Mars missions [7], and to estimate the thermally-driven wind speeds for wind resource assessment. Previous investigations report predicted surface wind speeds of 2–10 m/s in the Mars Pathfinder (MPF) rover site [8], 16 m/s in the Mars 2020 Perseverance rover site [9], and 17 m/s in Arsia Mons [1]. Wind gusts of above 30 m/s may occur on Mars [10], and peaks of 14–19 m/s were measured in the Insight and Viking Lander 2 (VL2) sites [11], while slope flow peaks of 10–15 m/s were measured in Aeolis Mons by the Rover Environmental Monitoring Station/Mars Science Laboratory (REMS/MSL) [12], where the Mars-WRF numerical model underpredicted the strength of daytime wind speeds by 2–4 m/s [13]. The wind power density for winds of 20–30 m/s would be 60–203 W/m^2, with the density from NASA's Martian atmospheric model. Hence, the same way that solar energy has potential to become an excellent source to power extended (multi-annual) Mars missions [13], wind energy, though being not optimum for first stages of human settlements on Mars, can become another interesting renewable energy source in the long term or as back-up for solar energy [11].

Slope winds in the area of Gusev Crater and Valles Marineris were simulated in [7]. Haberle et al. [14] developed a model for studying the winds in the Viking Lander 1 (VL1) landing site. VL1 data include a single profile of wind and temperature from 1.5 to 4 km height, and their diurnal variations at 1.6 m above ground level (AGL). The predicted model winds were able to match the wind surface data or wind vertical profiles, but not both simultaneously. The best agreement was obtained using a slope magnitude and/or direction different from the reported values. However, the model was able to reproduce the shape, phase, and sense of rotation of the surface wind hodograph at each site. These simulations included nocturnal LLJ, which may be common on Mars, and a negative feedback between the dust and surface stress.

Martian PBL phenomena were also studied using Prandtl's theory, a 2D mesoscale model, and VL1 data [1]. The model used turbulence and dynamics schemes validated for Earth, while the radiation and surface schemes were modified for Mars. Relevant findings from this work regarding katabatic winds are: 1) *During moderate prevailing large-scale wind:* Nocturnal LLJ are similar to those on Earth, but higher up (at 1 km), due to inertial oscillations after the rapid collapse of thermal turbulence at sunset (and thus LLJ are expected to exist over flat and over sloping regions), with some contribution from slope winds over sloping regions (very common on Mars): slope winds added 15–20% to the LLJ super-geostrophy of 3 m/s in VL1. 2) *During weak, large-scale wind:* Strong, regular drainage flows with strong vertical shear develop at nighttime down Martian slopes, as slopes are colder than the air, with peaks at ≈100 m height. For steep slopes, these winds can reach high speed (*e.g.*, 17 m/s in Arsia Mons). For fixed slope angle and no geostrophic wind, maximum drainage flow speeds are expected at latitude 25–35°. As regards to anabatic winds, the typical afternoon up-slope winds are vertically homogeneous, well-mixed up to 2–3 km (during daytime, the convective PBL grows up to 4–5 km in the late afternoon) and weak (1–4 m/s in magnitude), even over relatively steep, large-scale slopes [1].

The diurnal cycles of surface wind near the MPF rover and the VL1 lander are complex, and a good prediction requires sufficient model resolution to adequately simulate the contributing slope flows in these regions, because, in many Martian sites, near-surface winds are dominated by slope flows of multiple scales. In turn, slope flows dramatically influence the diurnal surface pressure cycle: surface winds from the Fifth-Generation Penn State University/National Center for Atmospheric Research (NCAR) Mesoscale Model adapted to Mars (MMM5) exhibit significant steering and channeling, which are a result of topographical slopes and thermally-induced flows [15].

Compared to investigations on Earth, one of the main challenges of the proposed numerical analysis is the widespread presence of suspended dust on Mars. The dust modifies significantly the radiative properties of the Martian atmosphere [8, 16, 17]. In daytime, the dust absorbs solar radiation, reducing the ground insolation and thus cooling the surface. At nighttime, dust infrared emission keeps the surface warm. Hence, the dust decreases the amplitude of the diurnal temperature variations, without strongly affecting the average surface temperatures. Conversely, dust has a key effect on atmospheric temperature. At sunlit latitudes, even for relatively clear air, the atmosphere at 20 km is 30 K warmer than if it was dust-free. The dust also enhances the horizontal temperature gradients on Mars, and thus the Martian atmospheric circulation [16]. OpenFOAM has been successfully applied for making CFD analyses of turbulent buoyant ABL flows [18, 19] and pollutant dispersion [20, 21, 22]. Therefore, it is expected that OpenFOAM is capable of simulating how suspended dust in the Martian atmosphere affects thermally-driven winds.

As a first step towards complex simulations of thermally-driven winds on Mars, and in order to validate the proposed methodology and the performance of OpenFOAM CFD for these purposes, slope winds are simulated in this work in an idealised 2D Martian mountain-valley system with realistic values of all relevant parameters.

2. NUMERICAL SETUP

To study the generation of thermally-driven winds during Martian diurnal cycles, OpenFOAM free open-source CFD software is used. The details of the methodology used here (such as the governing equations, the solver used, the assumptions made, etc.) is described in-depth in [5, 6], where the same geometry of a 2D 20º slope with valley was used. Among the OpenFOAM solvers for heat transfer analysis applicable for our research, *buoyantBoussinesqPimpleFoam* was chosen, a transient solver for buoyant, turbulent flow of incompressible fluids, which uses Navier-Stokes equations with Boussinesq approximation.

Figure 1 shows the mesh of the studied mountain-valley configuration, with the dimensions of the domain and the applied boundary conditions. A mesh of $254 \times 1 \times 500$ elements has been used, with uniform horizontal size of around 7 m and vertical size increasing from 0.11 m in the first layer on the slope and flat part to 27.6 m near the top area.

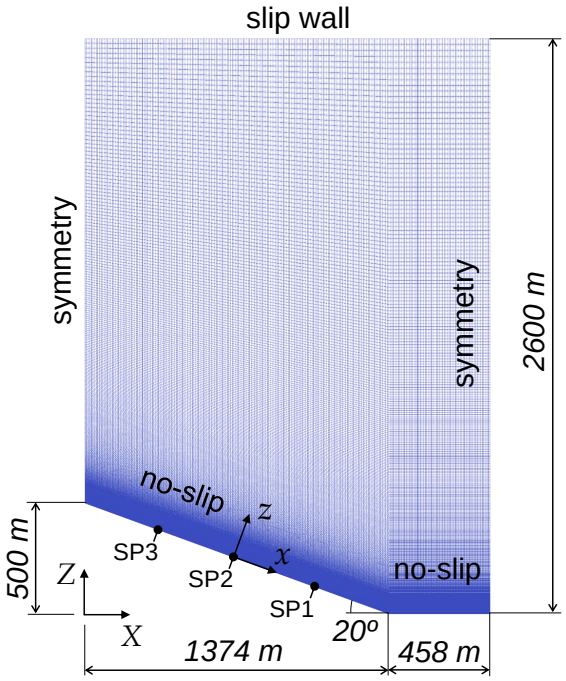

Figure 1. Mountain-valley geometry and mesh

To simulate the change of temperature due to the Martian diurnal cycle, a transient temperature profile was applied as boundary condition on the ground no-slip walls. The whole study considers as time period a sol (solar day on Mars, approximately 24.6 h), and the corresponding hours within a sol (Martian hours, h_M) are represented in all figures. The temperature profile was obtained by applying an analytical fitting to temperatures measured at 2 m on Mars [23]:

$$T(t) = 220.85 + 24.43 \sin(2\pi t/T_M - \pi) \quad [\mathrm{K}] \quad (1)$$

where $T_M = 88\,775$ s, giving an acceptable goodne ss of the fitting ($R^2 = 0.9704$). The temperature measurements and corresponding fitting can be seen in Figure 2. It is important to remark that the hours used in this and the subsequent plots are not terrestrial hours but Martian hours h_M, *i.e.*, the result of dividing a Martian sol in 24 identical time slots. Finally, mean temperatures of the Martian surface air are usually ≈220 K [1, 2, 8]. In his work, the mean temperature obtained in the fitting (220.85 K) is set as initial temperature in the computational field.

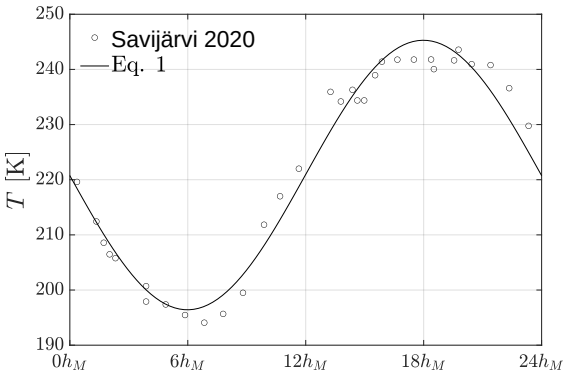

Figure 2. Surface temperature vs time (in Martian hours) for a Martian sol: measurements at 2 m [23] and corresponding analytical fit (Eq. 1)

Apart from correctly adjusting the temperature profile, the thermophysical and transport properties need to be correctly defined in the OpenFOAM setup. The most important simulation parameters are summarised in Table 1.

Table 1. Simulation parameters

Parameter	Value and units
μ	1.422×10^{-5} kg m^{-1} s^{-1}
ν	1.0868×10^{-3} m^2 s^{-1}
Pr	1
Pr_t	3
β	4.762×10^{-3} K^{-1}
R'	192 J kg^{-1} K^{-1}
M	0.0433 kg mol^{-1}
c_p	860 J kg^{-1} K^{-1}
g	3.71 m s^{-2}
p	800 Pa
z_0	0.01 m

LES studies have mostly focused on idealised numerical experiments on Mars PBL, and have produced plausible results with respect to the limited observations available [2]. LES distinguishes between the large eddies in the flow, which are mainly determined by the geometry of the problem under study, and the smaller eddies that tend to be more universal. A filter is applied so that scales smaller than the filter size are removed from the variables, and their effect on the resolved scales is modelled by means of a turbulence model. This is the turbulence model chosen here, with a Smagorinsky closure [3, 24]. Open-

FOAM default model coefficients are used.

The simulation was run for 2 sols on 16 cores (of 8 GB of DDR4-2666 ECC RAM each) of a Dual AMD EPYC™ 7001 Series Processors. The computational time needed to run a Martian sol of simulation time (887 750 time steps) is of around 5.4 days.

3. RESULTS

Figure 3 shows the along-slope flow maximum velocity u_{max} vs time, at different along-slope positions: 25% (SP1), 50% (SP2), and 75% (SP3) from the mountain base. As observed in similar studies on Earth [25], the katabatic flow (positive u_{max}) reaches lower along-slope velocities in absolute terms than the anabatic flow (≈3 vs ≈6 m/s, respectively). The order of magnitude of these values is in line with earlier works in Martian environments [1]. In the katabatic phase, u_{max} is rather constant in the lower part of the slope (SP1 and SP2), but it is ≈34% lower in the upper slope part (SP3), as in [26]. In the anabatic phase, there is a clear increase in flow velocity when going up the slope, with u_{max} at SP3 being twice the one at SP1. During this phase, velocity oscillations with time are also present, while the katabatic phase results are much more regular. Finally, note that the u_{max} value appears to be delayed in time from SP1 to SP3 in the katabatic phase: it occurs before the minimum temperature imposed as BC in the bottom of the slope, and increasingly later as we go up the slope. As for the anabatic case, the maximum value of u_{max} (in absolute value) is harder to identify due to the mentioned oscillations but seems more independent (in time) of the location on the slope.

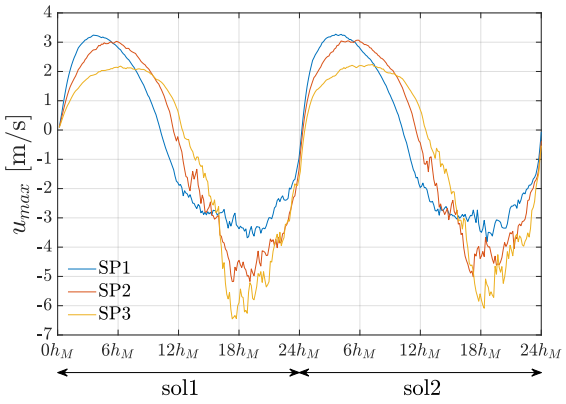

Figure 3. Maximum along-slope velocity u_{max} vs time (in Martian hours) at different positions along the slope

Figures 4 and 5 respectively show the flow velocity magnitude U at 3 h_M (katabatic phase) and at 18 h_M (anabatic phase) of the second sol. In the katabatic phase, a main descending flow is observed on the slope, while the rest of the domain remains rather still, being the obtained flow velocities in general much lower than in the anabatic phase. In Fig. 5, there is a main recirculation vortex confined in the top part of the fluid domain, which should not affect significantly the development of the anabatic flow, as also commented in [27] and studied for similar simulations on Earth in [5, 6]. Future simulations will consider additional computational domain heights H_D to confirm this. Several minor vortexes are also observed, explaining the velocity oscillations observed in Fig. 3.

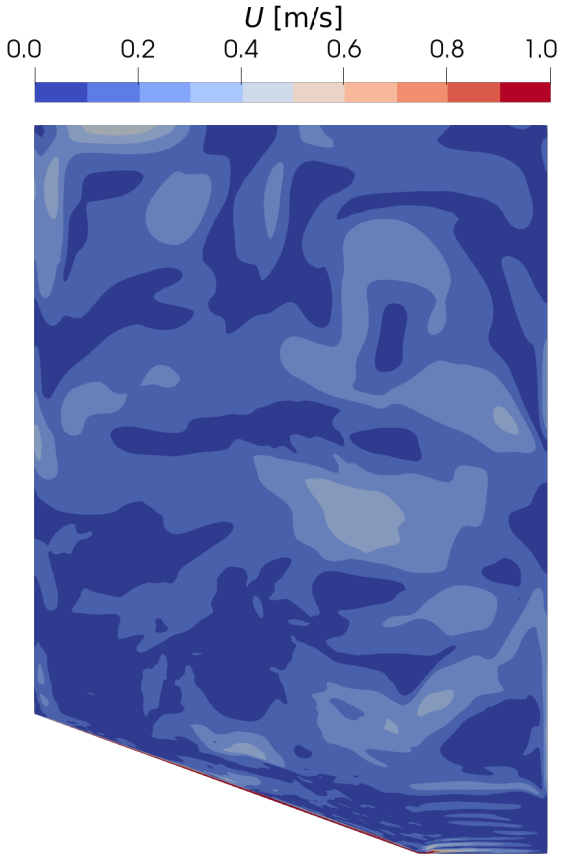

Figure 4. Katabatic: velocity U at 3 h_M for sol2

Figure 6 shows the along-slope flow velocity u vs time, at different slope-normal distances z, at mid-slope. In the katabatic phase, where u is lower, it is also remarkable that u decreases faster with z. This is likely because the temperature difference between the atmosphere and slope ΔT is larger in absolute terms for the anabatic case, as it is shown in Figure 8. Fig. 6 also shows that, for the katabatic case, u_{max} (≈3 m/s) is obtained right above $z = 1$ m, at $z = 5$ m, u is only ≈1 m/s, and for $z > 5$ m, u is close to zero. In the anabatic phase, again, u shows more oscillations, but it is clear that the decrease of u with z is slower than in the katabatic phase, being u virtually identical at $z = 2.5$ and 5 m, for example. This happens though the flow temperature is noticeably different at those z values, as seen in Figure 7, which shows the temperature T vs time, at different slope-normal distances at mid-slope. This figure shows that the time evolution of T is quite similar for all values of z, except, to some extent, for $z = 2.5$ m. Apart

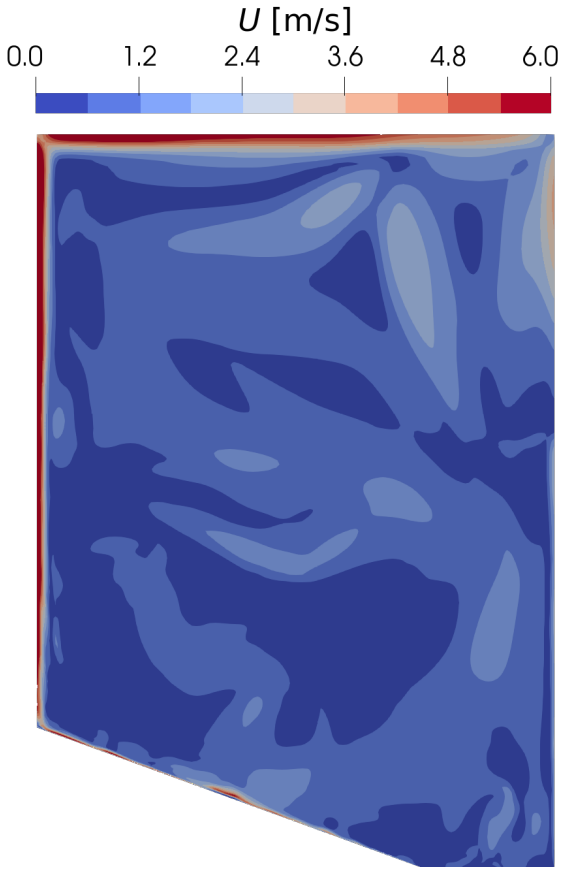

Figure 5. Anabatic: velocity U at 18 h_M for sol2

from the steep decrease of T for z from 0 to 2.5 m, it can also be seen how the original sinusoidal temperature profile (with time), imposed as BC, is lost almost immediately. This behaviour is quite different from the velocity profiles, which do retain a sinusoidal profile.

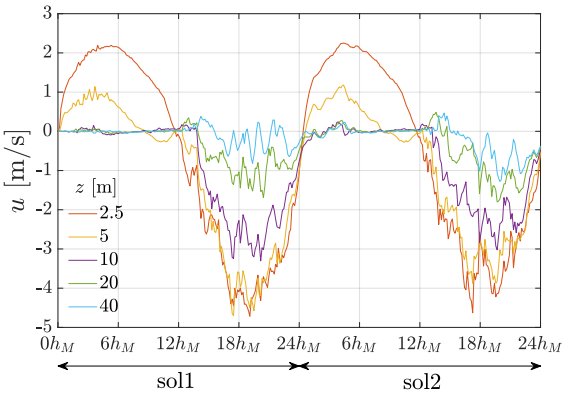

Figure 6. Along-slope velocity u vs time (in Martian hours) at different z-distances at mid-slope

Figures 8 and 9 show the along-slope velocity u and temperature difference ΔT as functions of the slope-normal distance z, at three positions along the slope (SP1, SP2, and SP3), for the katabatic (at 3 h_M) and anabatic (at 18 h_M) cases for sol2. For the katabatic case, though all ΔT profiles are quite similar up to z = 5 m (showing the already observed steep decrease of T), the steepest ΔT profile at SP3 leads to a quite lower u profile. As also seen in Fig. 3, velocity profiles at SP1 and SP2 are very similar, especially at low values of z. For z > 5 m, the profiles of u and ΔT at SP2 and SP3 become very similar, while the profiles at SP1 show significant discrepancies, particularly in ΔT, which might be due to the effect of the flat valley at the bottom of the slope. To be able to ascertain this, future work will study the influence of different valley widths on the results. However, this does not mean that the results presented here-in are not valid, given that the studied geometry may perfectly correspond to real geometries, as valleys with many different widths can be found on Mars. For the anabatic flow, it can be seen that, on the one hand, the temperature decreases more slowly at SP3 than at SP1 and SP2, leading to higher values of u for z > 2 m, and the peak position (*i.e.*, the position of u_{max}) rising to higher slope-normal distances. On the other hand, the slope-normal profiles of u and ΔT are very similar at SP1 and SP2.

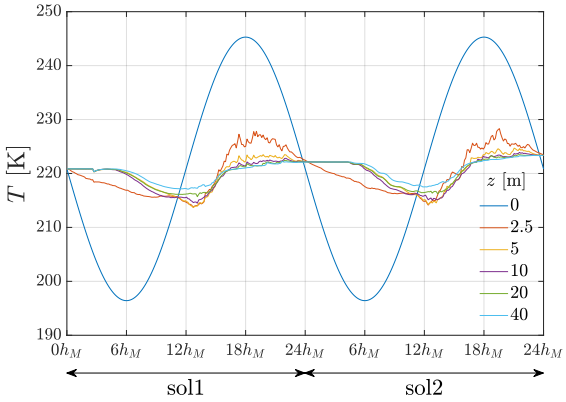

Figure 7. Temperature T vs time (in Martian hours) at different z-distances at mid-slope

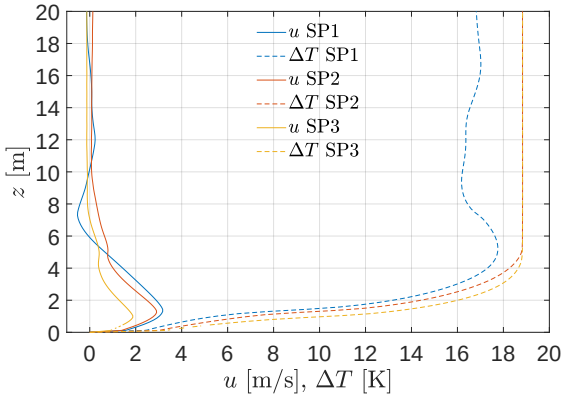

Figure 8. Katabatic: along-slope velocity u and ΔT profiles vs z-distance at 3 h_M for sol2

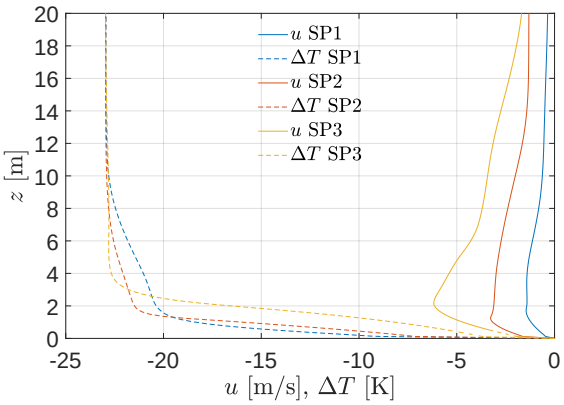

Figure 9. Anabatic: along-slope velocity u and ΔT profiles vs z-distance at 18 h_M for sol2

4. CONCLUSIONS

This work presents a preliminary study of numerical simulations performed with OpenFOAM, which proves its validity for generating slope winds in a Martian environment. The obtained velocity values are in line with previous investigations, showing higher magnitudes of the along-slope velocity in the anabatic case than in the katabatic one. The temperature gradient decreases rapidly from the ground, and thus the most significant along-slope flow velocities are basically observed just below slope-normal distances of 5 and 10 m for the katabatic and anabatic phases, respectively. The position along the slope also shows distinct effects on the flow velocity in the katabatic and anabatic phases.

Future work will compare LES with RANS turbulence models (such as k–ε, very common for simulating ABL flows on Earth [28]), and validate the choice of domain height and mesh size (depending on the chosen turbulence models). In a further step, interaction between geostrophic wind and slope wind may be simulated to study the influence of the geostrophic wind on the total generated wind. Finally, the effect of the Martian dust may be included into the simulations. This, considering realistic Martian geometries, could help assessing the possibility of using wind energy as an additional source to solar energy during long-term Martian missions.

ACKNOWLEDGEMENTS

This work has been supported by the project PID2019-105162RB-I00 funded by MCIN/AEI/10.13039/501100011033 and by the project 2017 SGR 1278 from the AGAUR from *Generalitat de Catalunya*.

REFERENCES

[1] Savijärvi, H. I., and Siili, T., 1993, "The Martian slope winds and the nocturnal PBL jet", *J Atmos Sci*, Vol. 50, pp. 77–88.

[2] Petrosyan, A., Galperin, B., Larsen, S. E., Lewis, S. R., Määttänen, A., Read, P. L., Renno, N., Rogberg, L. P., Savijrvi, H., Siili, T., Spiga, A., Toigo, A., and Vázquez, L., 2011, "The Martian atmospheric boundary layer", *Rev Geophys*, Vol. 49, p. RG3005.

[3] Cao, S., Wang, T., Ge, Y., and Tamura, Y., 2012, "Numerical study on turbulent boundary layers over two-dimensional hills - Effects of surface roughness and slope", *J Wind Eng Ind Aerodyn*, Vol. 104, pp. 342–349.

[4] Bhuiyan, A. A., Karim, R. M., Hart, J. T., Rahman, M. M., and Naser, J., 2016, "Experimental and numerical investigation of coherent structure dynamics on mass transfer in a separated cavity flow", *Exp Therm Fluid Sci*, Vol. 76, pp. 146–162.

[5] Athota, R. B., Rojas, J. I., Arias, S., and Montlaur, A., 2022, "Simulations of thermal wind formation in idealised mountain-valley systems using OpenFOAM", Available at SSRN: `https://ssrn.com/abstract=4086430` or `https://dx.doi.org/10.2139/ssrn.4086430`.

[6] Rojas, J., Arias, S., and Montlaur, A., 2022, "Comparison of OpenFOAM turbulence models for numerical simulation of thermally-driven winds", *Conference on Modelling Fluid Flow (CMFF'22)*, Budapest, Hungary.

[7] Justus, C. G., Duvall, A., and Keller, V. W., 2006, "Validation of Mars Global Reference Atmospheric Model (Mars-GRAM 2001) and planned new features", *Adv Space Res*, Vol. 38, pp. 2633–2638.

[8] Haberle, R. M., Joshi, M. M., Murphy, J. R. Barnes, J. R., Schofield, J. T., Wilson, G., Lopez-Valverde, M., Hollingsworth, J. L., Bridger, A. F. C., and Schaeffer, J., 1999, "General circulation model simulations of the Mars Pathfinder atmospheric structure investigation/meteorology data", *J Geophys Res*, Vol. 104, pp. 8957–8974.

[9] Pla-García, J., Rafkin, S. C. R., Martinez, G. M., Vicente-Retortillo, A., Newman, C. E., Savijärvi, H., de la Torre, M., Rodriguez-Manfredi, J. A., Gómez, F., Molina, A., Viúdez-Moreiras, D., and Harri, A.-M., 2020, "Meteorological predictions for Mars 2020 Perseverance Rover landing site at Jezero Crater", *Space Sci Rev*, Vol. 216, p. 148.

[10] Wilson, C. F., 2003, "Measurement of Wind on the Surface of Mars", Ph.D. thesis, University of Oxford, Linacre College.

[11] Schorbach, V., and Weiland, T., 2022, "Wind as a back-up energy source for mars missions", *Acta Astro*, Vol. 191, pp. 472–478.

[12] Soria-Salinas, A., Zorzano, M. P., Mantas-Nakhai, R., and Martín-Torres, J., 2020, "Wind retrieval from temperature measurements from the Rover Environmental Monitoring Station/Mars Science Laboratory", *Icarus*, Vol. 346, p. 113785.

[13] Newman, C. E., Gomez-Elvira, J., Marin, M., Navarro, S., Torres, J., Richardson, M. I., Battalio, J. M., Guzewich, S. D., Sullivan, R., de la Torre, M., Vasavada, A. R., and Bridges, N. T., 2017, "Winds measured by the Rover Environmental Monitoring Station (REMS) during the Mars Science Laboratory (MSL) rover's Bagnold Dunes Campaign and comparison with numerical modeling using MarsWRF", *Icarus*, Vol. 291, pp. 203–231.

[14] Haberle, R. M., Houben, H. C., Hertenstein, R., and Herdtle, T., 1993, "A boundary-layer model for Mars: Comparison with Viking Lander and entry data", *J Atmos Sci*, Vol. 50, pp. 1544–1559.

[15] Tyler Jr, D., Barnes, J. R., and Haberle, R. M., 2002, "Simulation of surface meteorology at the Pathfinder and VL1 sites using a Mars mesoscale model", *J Geophys Res*, Vol. 107, pp. 2–1–2–16.

[16] Forget, F., 2007, "Water and Climates on Mars", *Lect Astrobiol Vol II, Adv Astrobiol Biogeophys*, Springer-Verlag, Berlin, Heidelberg, pp. 103–122.

[17] Conrath, B. J., Pearl, J. C., Smith, M. D., Maguire, W. C., Christensen, P. R., Dason, S., and Kaelberer, M. S., 2000, "Mars Global Surveyor thermal emission spectrometer (TES) observations: Atmospheric temperatures during aerobraking and science phasing", *J Geophys Res*, Vol. 105, pp. 9509–9519.

[18] Bautista, M. C., 2015, "Turbulence Modelling of the Atmospheric Boundary Layer over Complex Topography", Ph.D. thesis, Université de Québec, École de Technologie Supérieure.

[19] Franke, J., Sturm, M., and Kalmbach, C., 2012, "Validation of OpenFOAM 1.6.x with the German VDI guideline for obstacle resolving micro-scale models", *J Wind Eng Ind Aerodyn*, Vol. 104–106, pp. 350–359.

[20] Flores, F., Garreaud, R., and Muñoz, R. C., 2014, "OpenFOAM applied to the CFD simulation of turbulent buoyant atmospheric flows and pollutant dispersion inside large open pit mines under intense insolation", *Comput Fluids*, Vol. 90, pp. 72–87.

[21] Ejtehadi, O., Mahravan, E., and Sohn, I., 2021, "Investigation of shock and a dust cloud interaction in Eulerian framework using a newly developed OpenFOAM solver", *Int J Multiphase Flow*, Vol. 145, p. 103812.

[22] Islas, A., Rodríguez-Fernández, A., Betegón, C., Martínez-Pañeda, E., and Pandal, A., 2022, "CFD simulations of turbulent dust dispersion in the 20 L vessel using OpenFOAM", *Powder Technol*, Vol. 397, p. 117033.

[23] Savijärvi, H. I., Martinez, G. M., Fischer, E., Renno, N. O., Tamppari, L. K., Zent, A., and Harri, A. M., 2020, "Humidity observations and column simulations for a warm period at the Mars Phoenix lander site: Constraining the adsorptive properties of regolith", *Icarus*, Vol. 343, p. 113688.

[24] Majander, P., and Siikonen, T., 2002, "Evaluation of Smagorinsky-based subgrid-scale models in a finite-volume computation", *Int J Numer Methods Fluids*, Vol. 40, pp. 735–744.

[25] Barcons, J., Avila, M., and Folch, A., 2019, "Diurnal cycle RANS simulations applied to wind resource assessment", *Wind Energy*, Vol. 22, pp. 269–282.

[26] Román-Gascón, C., Yagüe, C., Arrillaga, J. A., Lothon, M., Pardyjak, E. R., Lohou, F., Inclán, R. M., Sastre, M., Maqueda, G., Derrien, S., Meyerfeld, Y., Hang, C., Campargue-Rodríguez, P., and Turki, I., 2019, "Comparing mountain breezes and their impacts on CO_2 mixing ratios at three contrasting areas", *Atmos Res*, Vol. 221, pp. 111–126.

[27] Cintolesi, C., Di Santo, D., Barbano, F., and Di Sabatino, S., 2021, "Anabatic Flow along a Uniformly Heated Slope Studied through Large-Eddy Simulation", *Atmos*, Vol. 12 (7).

[28] Balogh, M. G., Parente, A., and Benocci, C., 2012, "RANS simulation of ABL flow over complex terrains applying an enhanced k-epsilon model and wall function formulation: Implementation and comparison for Fluent and OpenFOAM", *J Wind Eng Ind Aerodyn*, Vol. 104–106, pp. 360–368.